

Supplementary Information for

**First-principles insights into chromium-induced oxide
phases in NiO**

Xiao Peng^{a,b}, Jianmin Chen^{a,b}, Xin Yan^{a,b}, Wentao Wu^c, Wang Zhu^{a,b}, Canying Cai^{a,b}, Yujing Liu^{d*}, Guangwen Zhou^{e*}*

^aSchool of Materials Science and Engineering, Xiangtan University, Xiangtan 411105, China

^bKey Laboratory of Low Dimensional Materials & Application Technology of Ministry of Education, Xiangtan University, Xiangtan 411105, China

^cChangjun High School of Changsha City, Changsha, 410013, China

^dYuhua Institute of Advanced Materials, Baoji Xigong Titanium Alloy Products Co., Ltd, Baoji, 721300, China

^eDepartment of Mechanical Engineering & Materials Science and Engineering Program, State University of New York, Binghamton, NY 13902, USA

**Corresponding authors: cyc@xtu.edu.cn (C. Cai); liuyujing@iamyuhua.com (X. Liu); gzhou@binghamton.edu (G. Zhou)*

Supplementary Figures:

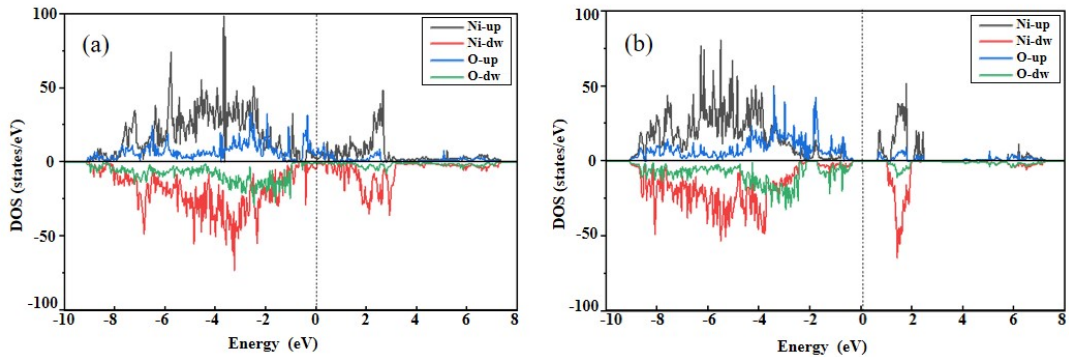


Fig. S1. PDOS for the NiO(111) surface with (a) Ni termination and (b) O termination. The O-terminated surface exhibits pronounced overlap between Ni and O states near the Fermi level, particularly within 0-3 eV, indicating strong Ni-O hybridization dominated by O 2p and Ni 3d states. This enhanced hybridization is accompanied by a reduced density of states at the Fermi level, reflecting improved electronic stability. In contrast, the Ni-terminated surface shows strong Ni-derived states near the Fermi level, characteristic of under coordinated surface Ni atoms and a less stable electronic configuration.

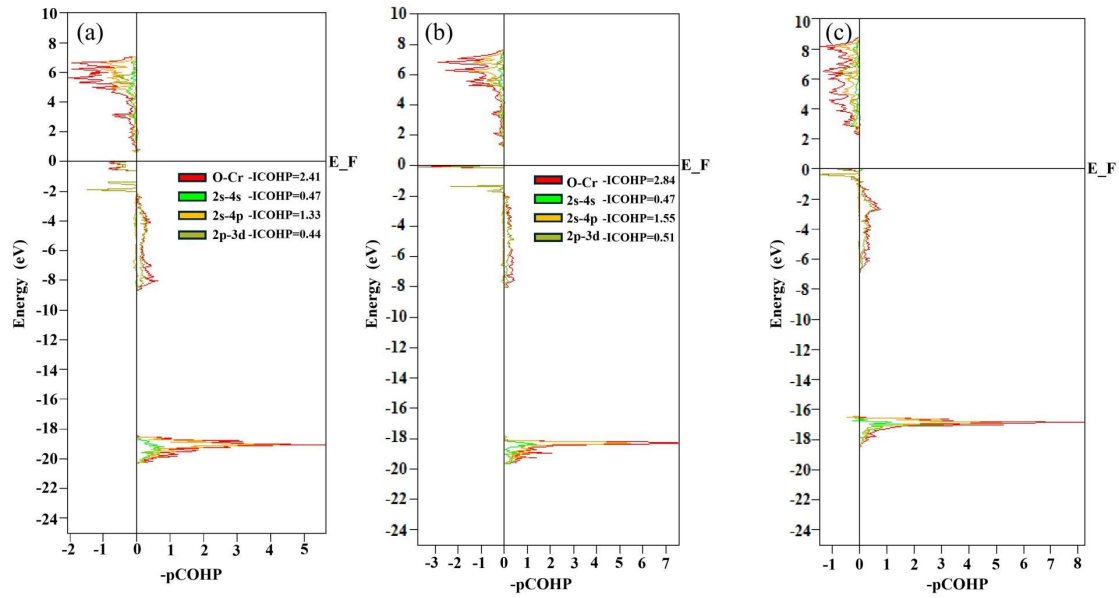


Fig. S2. COHP diagrams of Cr-O bonds. (a-c) COHP diagrams for a single Cr atom segregated at different sites (sub-subsurface, subsurface, and surface) of NiO(100). In the energy range from 0 to -8 eV, the bonding interactions are dominated by O 2p-Cr 3d hybridization, whereas deeper states between -21 and -16 eV arise primarily from O 2s-Cr 4p and O 2s-Cr 4s hybridization. As the Cr atom migrates toward the surface, the O 2p-Cr 3d and O 2s-Cr 4s interactions progressively strengthen, while the O 2s-Cr 4p interaction increases at the subsurface and subsequently weakens at the surface.

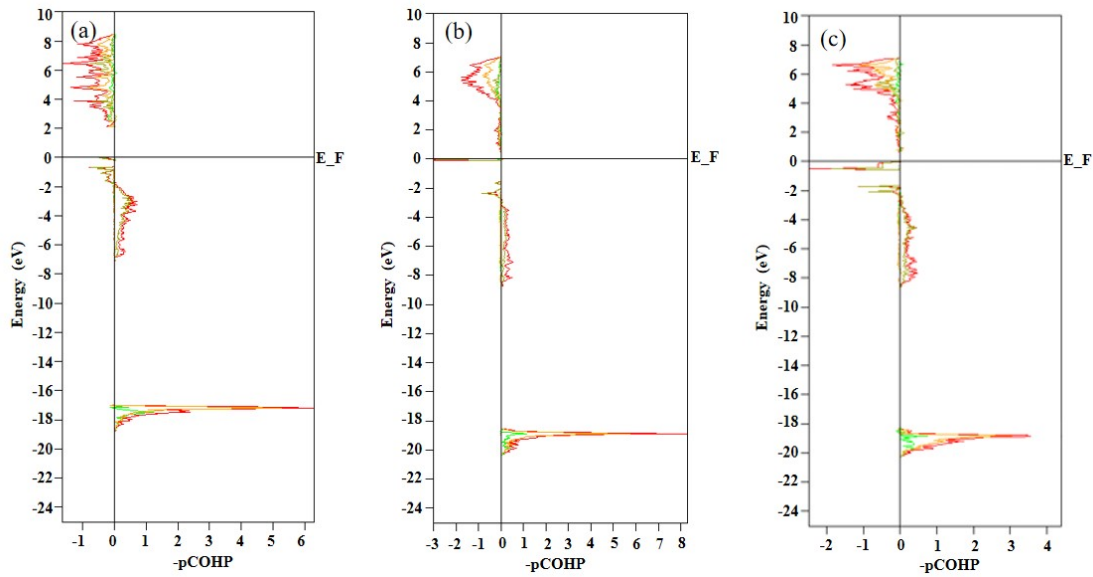


Fig. S3. COHP diagrams of Cr-O bonds. (a-c) COHP diagrams for two Cr atoms at different segregation configurations of NiO(100): (a) both in subsurface sites, (b) one in the subsurface and one on the surface, and (c) both on the surface. In the energy range from 0 to -8 eV, the interactions are dominated by O 2p-Cr 3d hybridization, whereas deeper states between -21 and -16 eV primarily arise from O 2s-Cr 4p and O 2s-Cr 4s hybridization. As the aggregated Cr atoms migrate toward the surface, the O 2p-Cr 3d and O 2s-Cr 4s interactions progressively strengthen, while the O 2s-Cr 4p interaction increases at the subsurface and subsequently weakens at the surface.

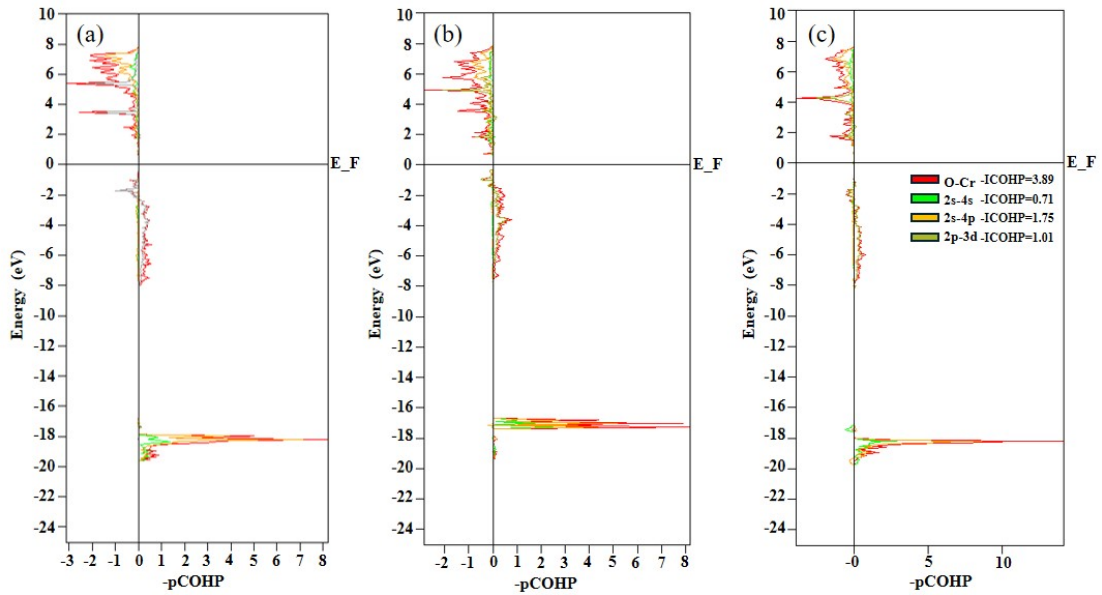


Fig. S4. COHP diagrams of Cr-O bonds. (a-c) COHP diagrams for a single Cr atom segregated at different sites (sub-subsurface, subsurface, and surface) of NiO(110). In the energy range from 0 to -8 eV, the bonding interactions are dominated by O 2p-Cr 3d hybridization, whereas deeper states between -21 and -16 eV primarily arise from O 2s-Cr 4p and O 2s-Cr 4s hybridization. As the Cr atom migrates toward the surface, the O 2p-Cr 3d and O 2s-Cr 4p interactions are progressively enhanced, while the O 2s-Cr 4s interaction initially weakens and subsequently strengthens., while the interaction between O2s-Cr4s first weakens and then strengthens.

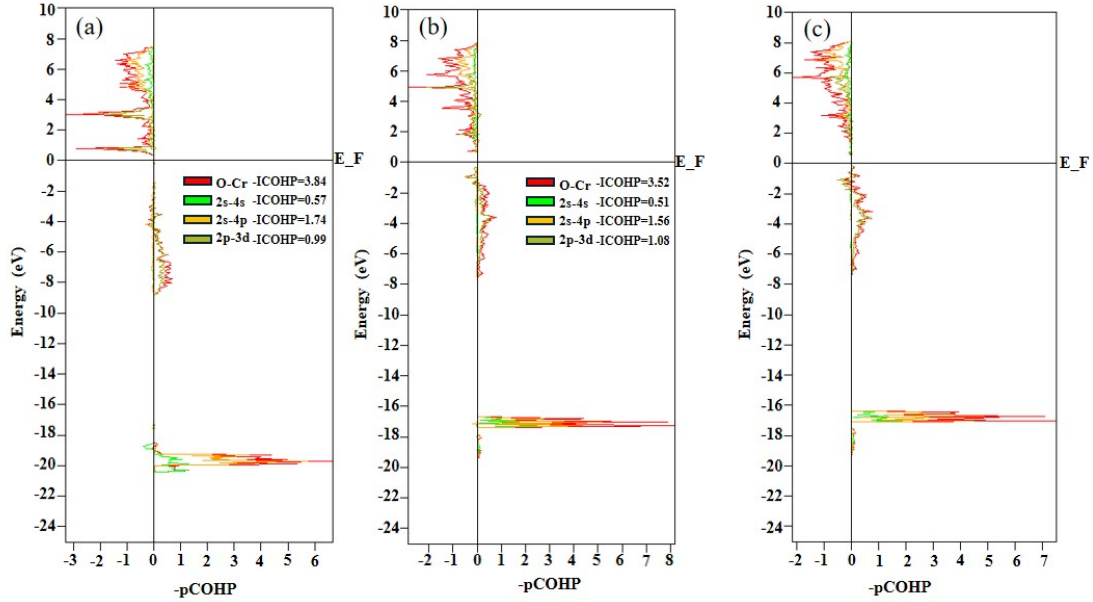


Fig. S5. COHP diagrams of Cr-O bonds. (a-c) COHP diagrams for two Cr atoms at different segregation configurations of NiO(111): (a) both in subsurface sites, (b) one in the subsurface and one on the surface, and (c) both on the surface. In the energy range from 0 to -8 eV, the bonding interactions are dominated by O 2p-Cr 3d hybridization, while deeper states between -21 and -16 eV arise primarily from O 2s-Cr 4p and O 2s-Cr 4s hybridization. As the aggregated Cr atoms migrate toward the surface, the O 2s-Cr 4s interaction remains relatively constant, whereas the O 2s-Cr 4p and O 2p-Cr 3d interactions initially weaken and subsequently strengthen.

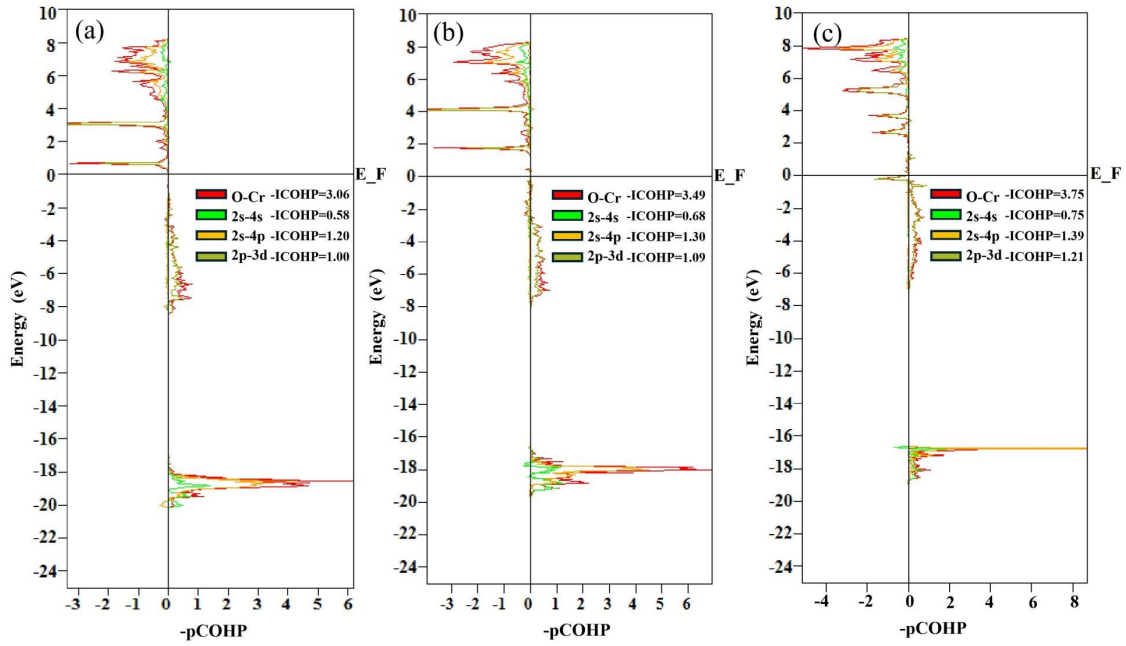


Fig. S6. COHP diagrams of Cr-O bonds. (a-c) COHP diagrams for a single Cr atom segregated at different sites (sub-subsurface, subsurface, and surface) of NiO(111). In the energy range from 0 to -8 eV, the bonding interactions are dominated by O 2p-Cr 3d hybridization, while deeper states between -21 and -16 eV primarily arise from O 2s-Cr 4p and O 2s-Cr 4s hybridization. As the Cr atom migrates toward the surface, these Cr-O orbital interactions are progressively strengthened, indicating enhanced bonding and increased surface stabilization.

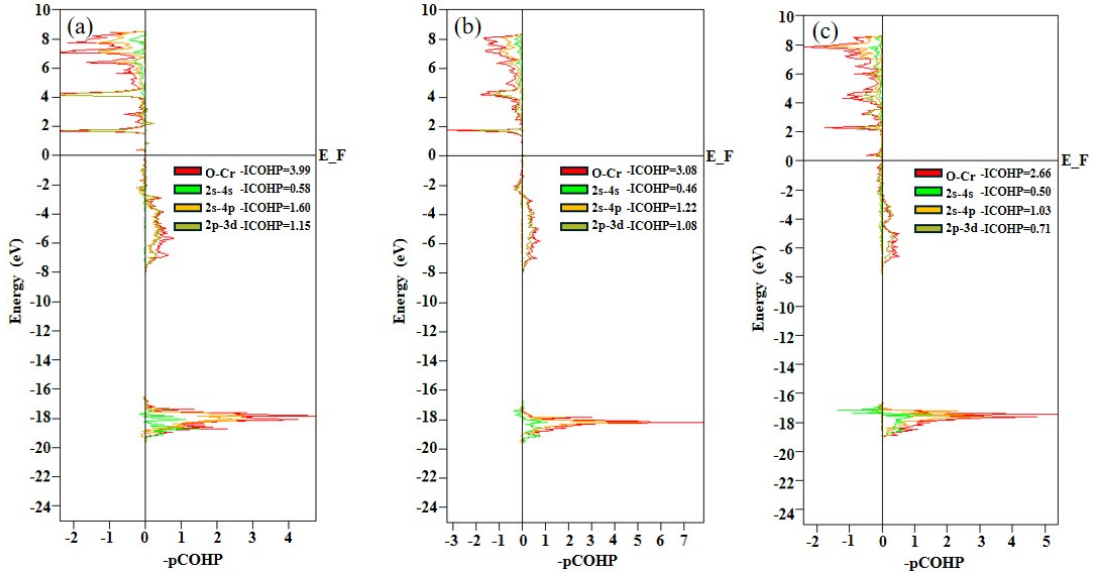


Fig. S7: COHP diagrams of Cr-O bonds. (a-c) COHP diagrams for two Cr atoms at different segregation configurations of NiO(111): (a) both in subsurface sites, (b) one in the subsurface and one on the surface, and (c) both on the surface. In the energy range from 0 to -8 eV, the bonding interactions are dominated by O 2p-Cr 3d hybridization, while deeper states between -21 and -16 eV primarily arise from O 2s-Cr 4p and O 2s-Cr 4s hybridization. As the aggregated Cr atoms migrate toward the surface, the O 2s-Cr 4s interaction initially weakens and subsequently strengthens, whereas the O 2s-Cr 4p and O 2p-Cr 3d interactions are progressively enhanced.

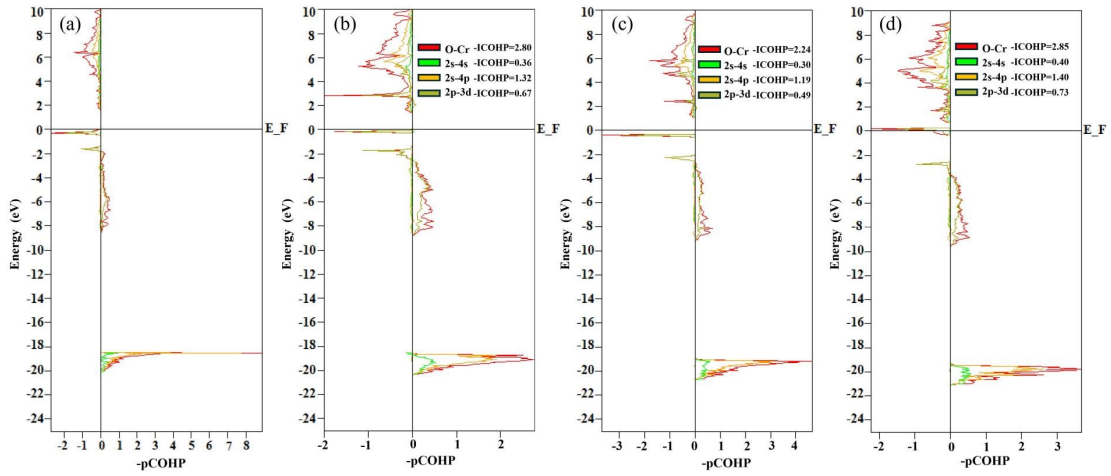


Fig. S8: (a-d) The COHP plots illustrate the primary interacting orbitals between Cr-O in the NiO bulk, in states where two or three Cr atoms are dispersed or aggregated, and the nearest neighboring O atoms. In the energy range from 0 to -8 eV, the bonding interactions are dominated by O 2p-Cr 3d hybridization, while deeper states between -21 and -16 eV primarily arise from O 2s-Cr 4p and O 2s-Cr 4s hybridization. Upon Cr aggregation, the O 2p-Cr 3d, O 2s-Cr 4p, and O 2s-Cr 4s interactions are all significantly enhanced compared to the dispersed configurations, indicating stronger cooperative Cr-O bonding in the aggregated states.